Contents

Chapter 1

Introduction

SHARP II+ is a near infrared camera which has been specially designed for the use with the adaptive optics system ADONIS, profiting from the experience gained with the speckle camera SHARP I operated at the NTT and a previous version of a dedicated adaptive optics camera SHARP II.

SHARP II+ is a camera for diffraction limited imaging in the spectral range from 1.1 to 2.45 μm, using a Rockwell NICMOS 3 array (HgCdTe, 256×256 elements) as detector and supplying three image scales of 35, 50 and 100 $mas/pixel$. A cold shutter allows to use integration times down to 20 ms for bright sources. A Lyot stop reduces the background radiation produced by the telescope and the optical components in the beam. For photometry, standard bandpass filters (J, H, K and K') are available. Low resolution spectroscopy is provided by a set of narrow band filters (R $\approx$ 100) at selected line positions and a CVF (Circular Variable Filter, R $\approx$ 60) for the 1.4 to 2.4 μm range. The CVF is also used as an order selector for two K-band Fabry-Perot etalons with spectral resolutions of 1000 and 2200 respectively. A wire grid polarizer can be inserted into the beam in front of the camera. For highest resolution imaging in J- and H-band, an atmospheric dispersion corrector is available.

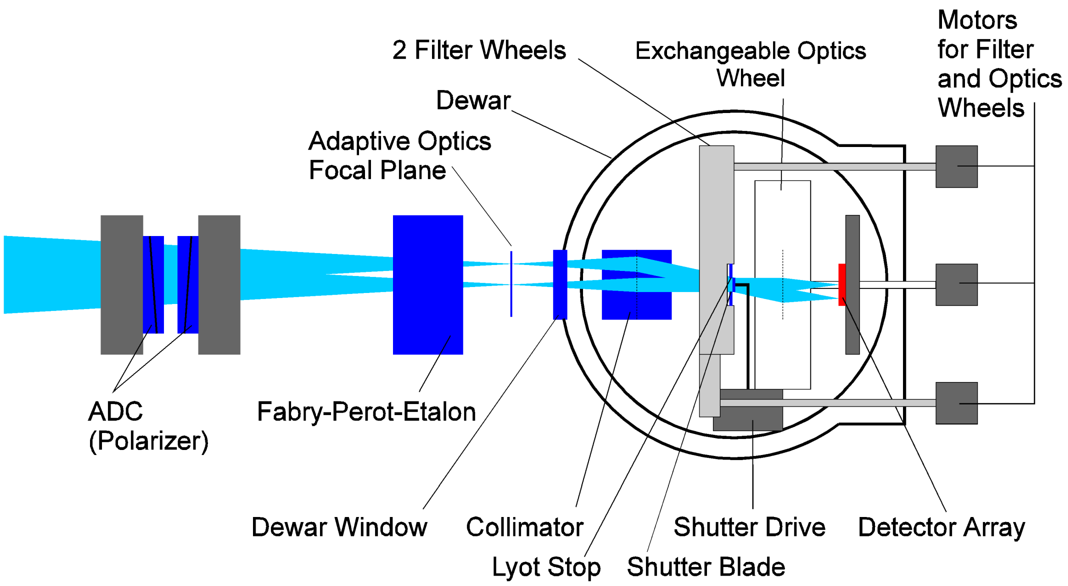

Figure 1.1: *The concept of SHARP II+*

Chapter 2

Technical description

2.1 Optics

2.1.1 Imaging optics

The SHARP II+ camera optics provides 3 different magnifications and a pupil imaging lens. The image scales and fields of view are summarized in table 2.1. The optical design takes special

Image scale	Field of view
35 $mas/pixel$	$9.0'' \times 9.0''$
50 $mas/pixel$	$12.8'' \times 12.8''$
100 $mas/pixel$	$25.6'' \times 25.6''$

Table 2.1: *Image scales and field of view*

care in the reduction of the background by placing a Lyot-stop (special aperture stop with a central obscuration to block radiation from the position of the telescope secondary mirror) at an intermediate pupil position within the camera. This intermediate pupil with a diameter of about 1.5 mm is generated by a collimator made of Barium Fluoride and the Schott IRG2 glass. Nearby this pupil position the different narrow- and broad-band filters and the shutter are placed. The different doublets mounted on the optics wheel behind the pupil provide the described image scales. While the doublets for the 35 and 50 $mas/pixel$ scale are manufactured from Barium Fluoride only, the doublet for the 100 $mas/pixel$ scale is achromatized like the collimator by a combination of Barium Fluoride an IRG2. Also mounted on this optic wheel, a doublet of two Zinc Selenide lenses images the pupil on the detector. This pupil imaging optics is used for the alignment of the camera to the optical axis of the adaptive optics bench. All the lens surfaces are coated for maximum transmission in the wavelength range from 1.1 to 2.45 μm. The overall transmission of the camera optics is about 10 % in the wavelength range from 1.1 to 2.45 μm.

2.1.2 Filter

SHARP II+ is equipped with 15 narrow-band filters, 4 broadband filters and one CVF (Circular Variable Filter).

Broad-band Filter

Table 2.2 summarizes the characteristics of the used broadband filters at the working temperature of 77 K. The transmission curves are shown in the appendix A.

Filter	50% - Wavelength in μm	50% - Wavelength in μm	Transmission
J	1.105	1.401	$\approx$ 75%
H	1.467	1.820	Peak 82%
K	1.988	2.366	Peak 76%
K'	1.993	2.316	Peak 91%

Table 2.2: *Characteristics of the broadband filters in SHARP II+*

Narrow-band Filter

Table 2.3 summarizes the characteristics of the narrow-band filters at the temperature of 77 K. The transmission curves are shown in appendix A.

Filter	Central Wavelength of filter in nm	Resolution	Transmission in %
Continuum	1068	107	61
HeI	1083	135	47
Pγ	1093	109	53
Continuum	1107	138	42
Continuum	1220	136	56
OII	1236	137	42
FeII	1256	105	48
Pβ	1281	142	56
Continuum	1296	144	55
Continuum	2044	120	69
HeI	2057	147	70
Continuum	2087	104	64
Continuum	2099	117	45
H_2 $\nu : 1-0$	2121	141	68
Continuum	2145	126	50

Table 2.3: *Characteristics of the narrow-band filters in SHARP II+*

Circular Variable Filter

A circular variable filter is an interference filter, where the thickness of the interference layer varies along an arc. For the CVF implemented in SHARP II+, the intrinsic resolution — the area of the CVF used to measure the transmission curve is small compared to a resolution element and the beam divergence is negligible — and its transmission are listed in table 2.4 for 3 wavelengths. Because the transmitted area of the CVF within the SHARP II+ camera is of finite size, the achieved spectral resolution (summarized in table 2.5) is somewhat smaller than the intrinsic resolution.

Wavelength in μ	Resolution $\frac{\lambda}{\delta\lambda}$	Transmission in %
1.319 μm	72	35
1.859 μm	67	69
2.399 μm	67	75

Table 2.4: *Intrinsic Resolution and transmission of the CVF*

Wavelength in μ	Resolution $\frac{\lambda}{\delta\lambda}$
1.523 μm	52
1.694 μm	56
2.117 μm	58
2.190 μm	63
2.253 μm	60

Table 2.5: *Resolution of the CVF in SHARP II+*

2.2 Detector

SHARP II+ is equipped with a NICMOS3 focal plane array from Rockwell International Corporation. Table 2.6 summarizes the detector characteristics. Beside the read noise of 38 electrons

Material	HgCdTe
Architecture	4 Quadrants, 128×128 Pixels each
Pixelsize	$40\ \mu m \times 40\ \mu m$
Quantum-efficiency Wavelength range of sensitivity	$\approx 60\%$ $0.8 \ldots 2.5\ \mu m$ at $77\ K$
Working temperature	$77\ K$
Read noise (reset read read)	$38.2\ e^-$
Conversion factor	$9.36\ e^-/ADU$
Pixel transfer function	$613\ e^-/mV$
Detector capacity	$0.0983\ pF$
Linearity range (deviation less than 1 %)	$204000\ e^-$
Potential well depth	$2.83 \times 10^5\ e^-$
Dark current	$5.79\ e^-/s \times e^{-\frac{t}{26.9s}}$
Number of dead pixels	351 (0.5%)

Table 2.6: *The Rockwell NICMOS 3 Detector in SHARP II+*

for a complete reset-read-read procedure (the read noise for a single readout is 27 electrons), the linearity range and the dark current are the most important characteristics. They are plotted in the figures 2.1 and 2.2. Figure 2.3 shows a map of the dead pixels. For all these dead pixels the quantum efficiency differs by more than 20 % from the median.

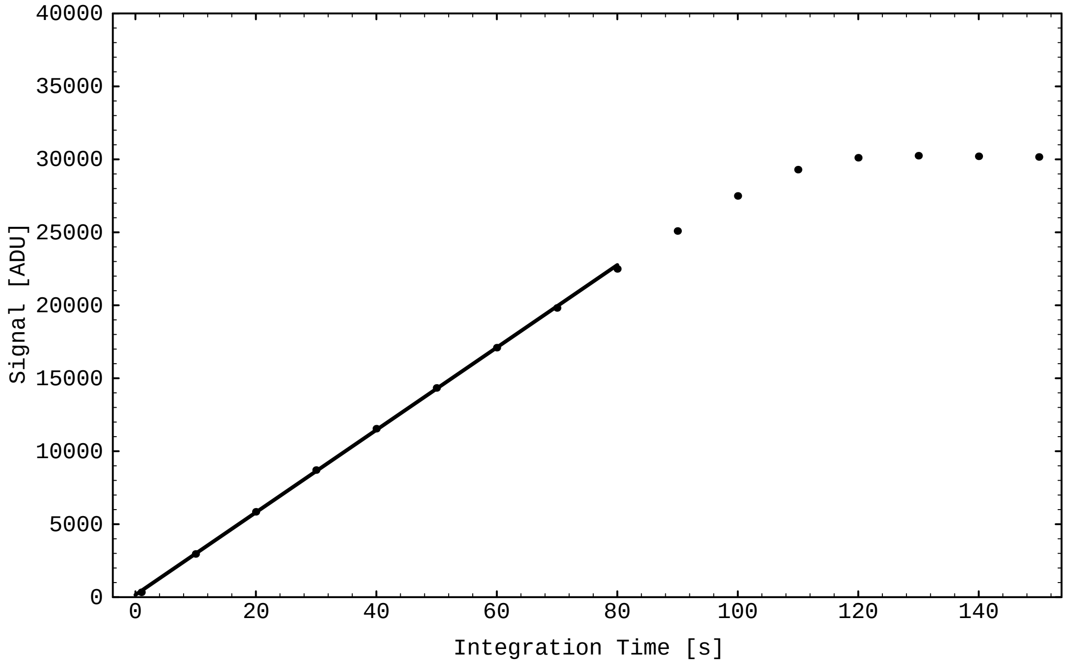

Figure 2.1: *Linearity of the detector*

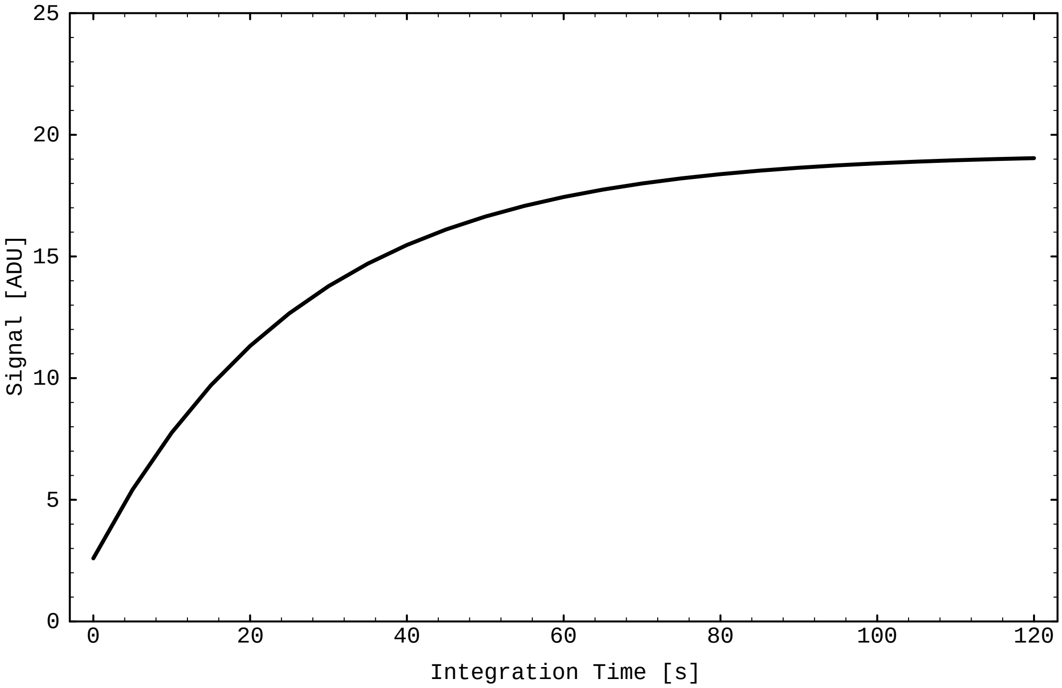

Figure 2.2: *Dark current*

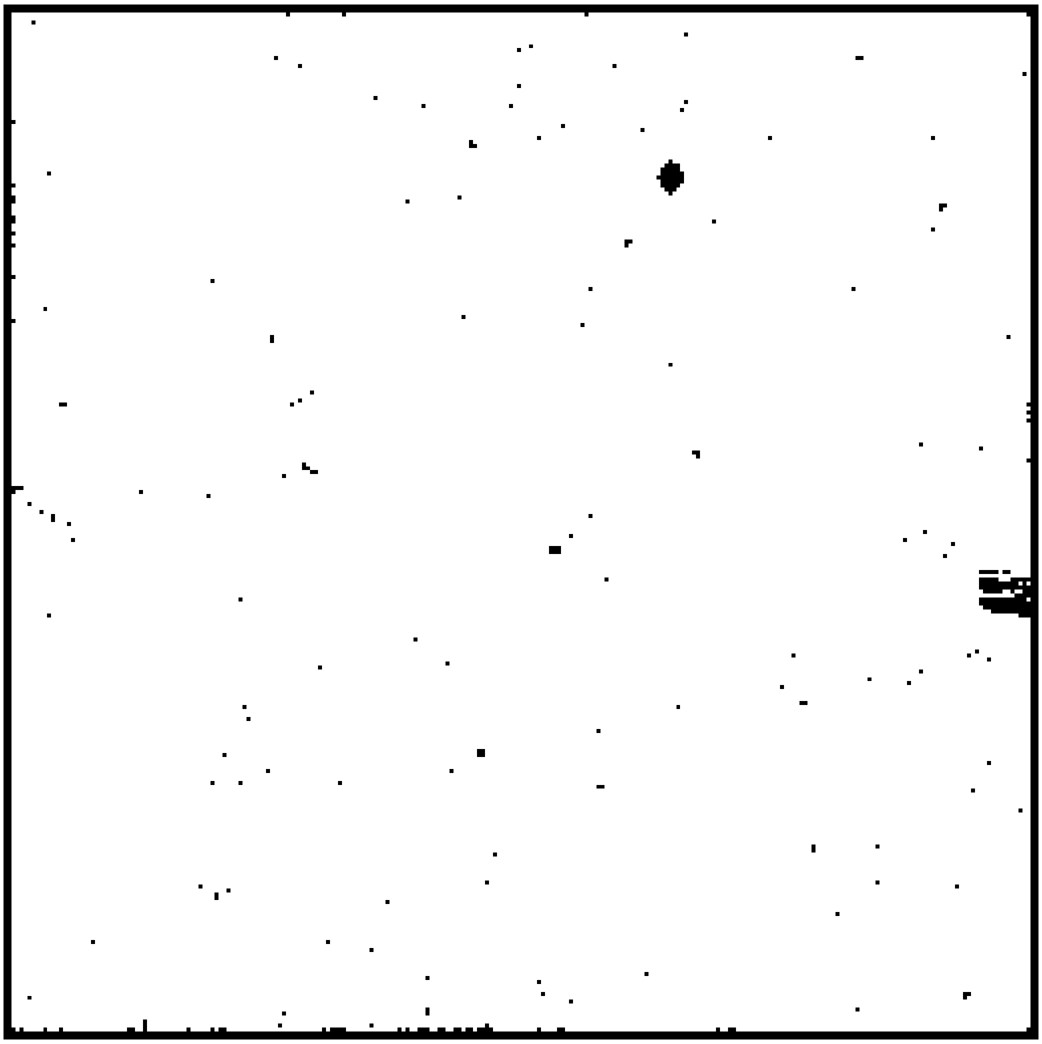

Figure 2.3: *Map of dead pixels. North is right and east is down*

2.3 Shutter

The shortest integration time achievable in the normal readout mode of the detector (reset read read) is limited to 400 ms. For shorter integration times a stepper motor driven shutter is implemented in SHARP II+. The shortest possible integration time is 20 ms. In both modes, the time spend on the readout procedure is about 900 ms.

2.4 Prefocal Optics

2.4.1 Fabry-Perot etalons

To obtain high resolution spectroscopy (R = 1000, 2200) in the K-band, two Fabry-Perot etalons can be mounted in front of the camera. Their finesse and the resolution for different wavelengths are tabulated in table 2.7 and 2.8. The transmission in the wavelength range from 1.9 to 2.4 μm is 85 % for the low resolution etalon and 65 % for the high resolution etalon. Figures 2.4 and 2.5 show the shift in passband across the field of view. Within the the recommended pixel-scale of 50 $mas/pixel$ (dashed lines), this shift is less than 0.2 nm for the low resolution etalon and less than 0.5 nm for the high resolution etalon.

λ in μm	Finesse F	Resolution
2.104	38	950
2.117	40	1000
2.171	42	1000
2.190	42	1000
2.253	48	1100
2.334	38	840

Table 2.7: *Finesse and resolution for the low resolution Fabry-Perot etalon*

λ in μm	Finesse F	Resolution
2.104	45	2200
2.117	46	2250
2.171	46	2200
2.190	46	2160
2.253	40	1840
2.334	33	1450

Table 2.8: *Finesse and resolution for the high resolution Fabry-Perot etalon*

2.4.2 Polarizer

Also a wire grid polarizer can be inserted into the beam in front of the camera. Its specifications are summarized in Table 2.9.

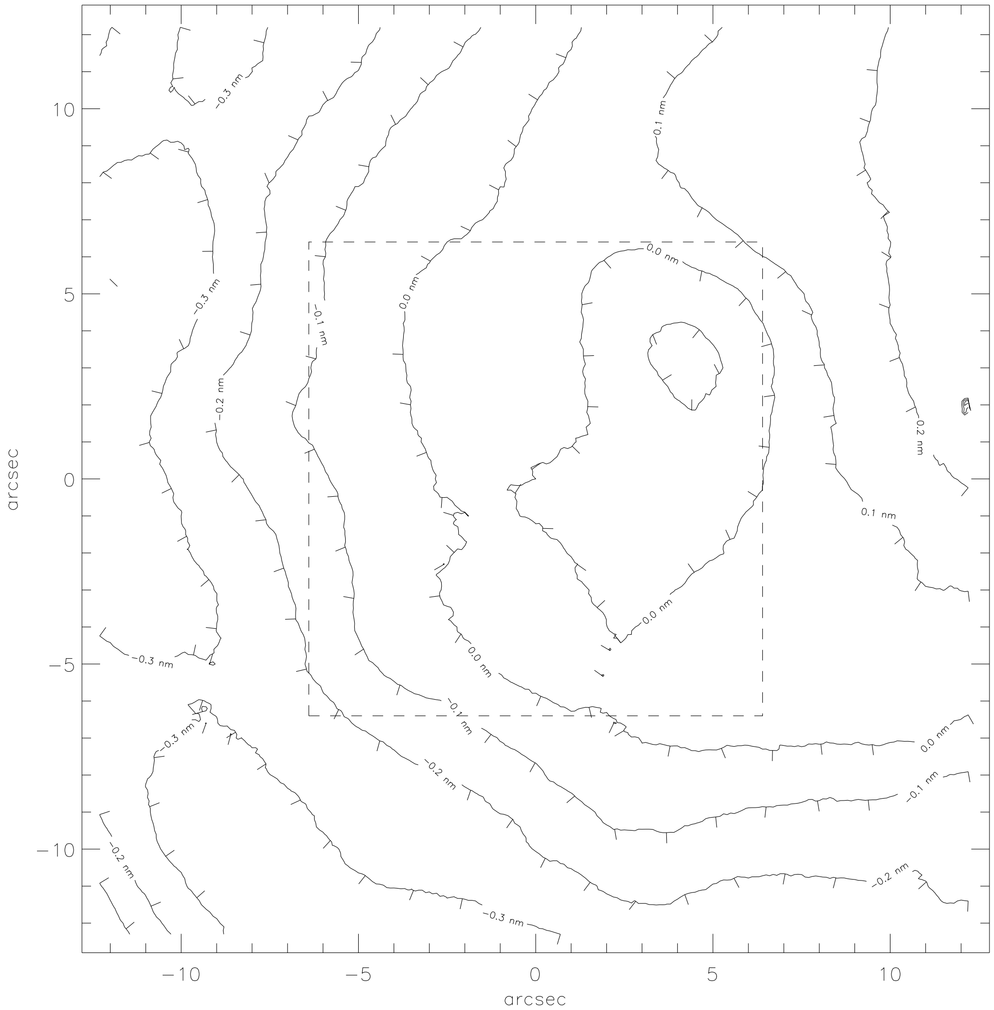

Figure 2.4: *Shift in passband for the low resolution Fabry-Perot etalon. The dashed lines represent the field of view in the* 50 *mas/pixel scale. The the short, perpendicular tick marks point "downhill". North is right and east is down*

Substrate	Calcium Fluoride
Spectral range	1 - 9 μm
Grid period	0.25 μm
Transmission for polarization perpendicular to the wire grid at 1.5 μm	83%
Transmission for polarization parallel to the wire grid at 1.5 μm	3 %
Degree of polarization at 1.5 μm	93 %

Table 2.9: *Specifications of the polarizer*

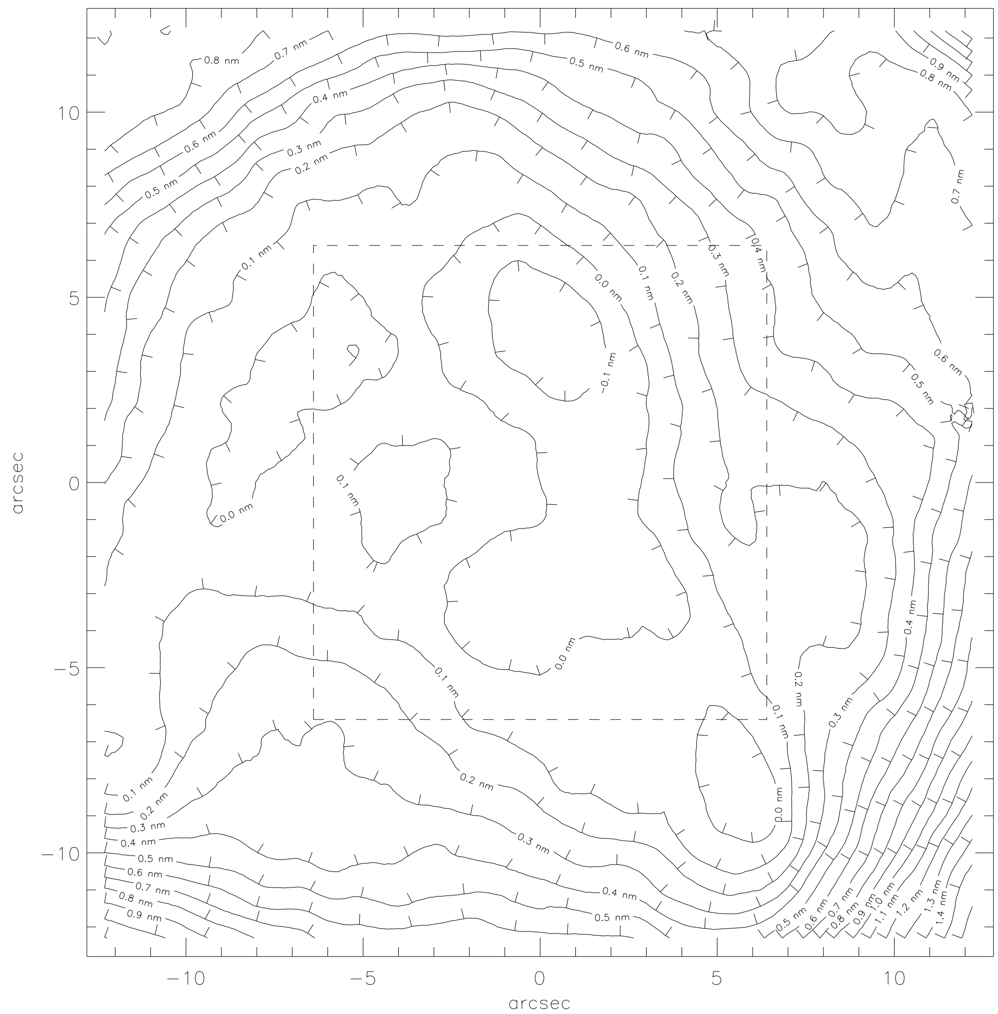

Figure 2.5: *Shift in passband for the low resolution Fabry-Perot etalon. The dashed lines represent the field of view in the* 50 *mas/pixel scale. The the short, perpendicular tick marks point "downhill". North is right and east is down*

2.4.3 Atmospheric dispersion corrector

The atmospheric dispersion prevents diffraction limited observation at higher zenith distances in J- and H-band. To correct this wavelength dependent aberration, an atmospheric dispersion corrector can be placed in front of the camera. Up to now, this instrument is only for experimental use. Figure 2.6 illustrates the correction for a zenith distance of 60°. This ADC is build of two pairs of prisms made of ZnSe and ZnS-Multispectral. Each pair of prisms is cemented. All the surfaces are coated for highest transmission. The average transmission of the complete ADC in the wavelength range from 1.1 to 2.45 μm is 95 %.

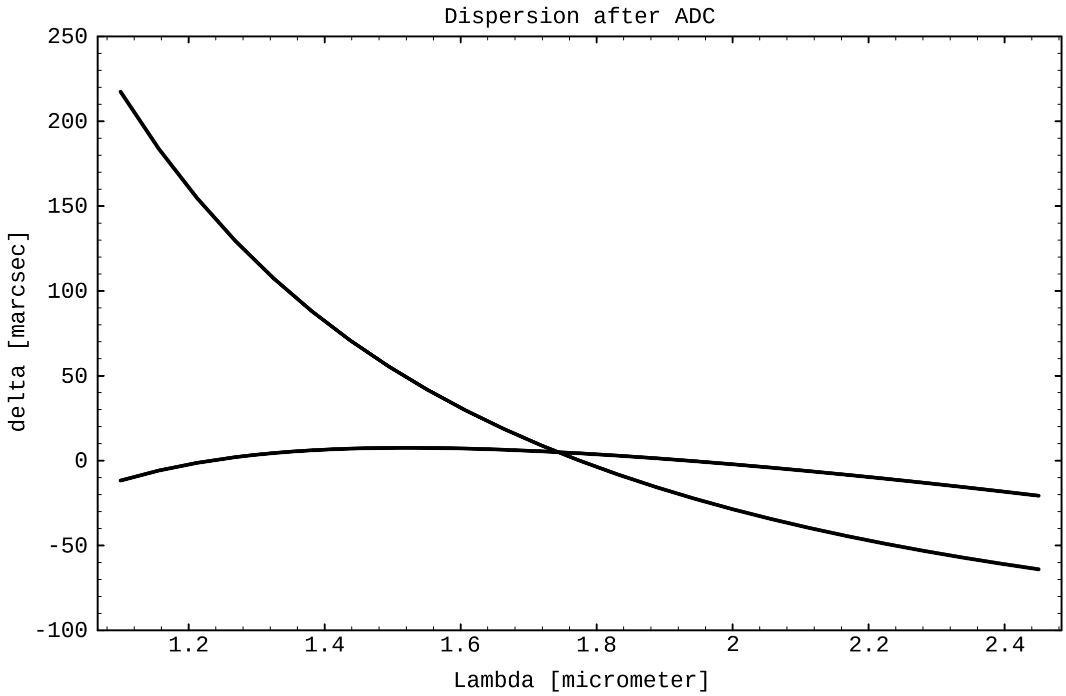

Figure 2.6: *Atmospheric dispersion at an zenith distance of* 60° *without correction and using an ADC*

Chapter 3

Observations

3.1 General remarks

The observer should be familiar with the techniques of near infrared observation:

- Sky-subtraction: For every frame of the astronomical object one sky frame should be recorded (pointing sequence programmable)
- Flat field correction: For every image scale and wavelength a flat-field should be generated (dome-flats, twilight-flats, etc.)
- Photometric calibration: Several photometric reference stars nearby the object of interest should be observed simultaneously

Because the correction of the atmospheric aberrations by adaptive optics is incomplete, full advantage from adaptive optics observations can be achieved only by deconvolution (Lucy-Richardson algorithm, maximum entropy deconvolution, etc.) with the point spread function. This point spread function is highly depending on the seeing conditions and the brightness of the reference star. Therefore, if there is no well separated reference star within the observed field, a separate observation of a nearby reference star of similar brightness is necessary.

3.2 Orientation of the field of view

On the observers screen, north is to the right and east is down. In the output FITS files, the first dimension is pointing towards north, the second dimension towards east.

3.3 Image scale

As already described in the technical description, the SHARP II+ camera provides three different image scales. For most observations the 50 $mas/pixel$ scale is recommended. When observing in K-band, this pixel scale provides full Nyquist sampling of the diffraction limited point spread function (3 pixels per FWHM). Even for J- and H-band, this pixel scale samples the point spread function accurately enough, when observing under average seeing conditions. For extraordinary seeing conditions or if the field of view is of minor interest, the 35 $mas/pixel$ scale is recommended. The 100 $mas/pixel$ scale with its larger field of view is very useful in the beginning of the observations for finding the object of interest within a crowded field. The larger field of view also helps the observer in searching for yet unknown objects and mapping larger areas on the sky. Beside this advantages, the 100 $mas/pixel$ scale has several disadvantages. First, there is vignetting of about 20 % towards the corner of the field of view. Second, in the present configuration the ADONIS field of view is somewhat too small for recording sky frames by moving the ON/OFF mirror. Third, there is an unavoidable reflection between the detector and the filters. The center of symmetry is at pixel (74,127). Table 3.1 summarizes the recommendations.

Pixel scale	Recommended purpose
35 $mas/pixel$	Observations in J- and H-band under excellent seeing conditions
50 $mas/pixel$	General purpose
100 $mas/pixel$	Search for faint objects and mapping of large areas

Table 3.1: *Pixel scale and recommended purpose*

3.4 Dead pixels

As showed in figure 2.3 in the technical description, there is an cluster of dead pixels located nearby the center of of upper-right (north-west) quadrant and at the right (north) edge of the detector. One should take care of this clusters, when positioning the object in the field of view.

3.5 Limiting Magnitude

The capability of detecting an astronomical object in an image is limited by the spatial noise in the background. The brightness of the faintest object which can be detected is called limiting magnitude. This limiting magnitude depends on the structure of the light-source to be detected, the shape of the point spread function and the criteria of the detection. Because the image correction by the adaptive optics is highly depending on the seeing conditions, the limiting magnitude also differs from observation to observation. The numbers presented here were calculated for average observing conditions, where 50% of the flux from the object is encircled in the following 50%-radii R50 (from “Report on Image Quality of the COME-On Plus Adaptive Optics Instrument (M13)” by E. Tessier from June 27, 1995):

- R50 = 0.500 arcsec for J-band
- R50 = 0.470 arcsec for H-band
- R50 = 0.315 arcsec for K-band

The calculations were carried out for a point-like object and a 5 σ detection (50 % of the overall flux of the object is 5 times the noise in the background signal within the area defined by the 50% radius). Depending on wavelength and pixel scale, the shot noise induced by the thermal background and dark current of the detector exceeds the readout noise after a certain integration time per individual frame. This integration times for background limited observations are summarized in table 3.2. For integration longer than the tabulated values, the brightness of the background limits the observations. The background brightness for the different filter bands are summarized in table 3.3. The figures 3.1 and 3.2 illustrate the results for integration times of one second and one minute per frame. The total integration time (abscissa) already includes the time to spend on sky observations.

	35 $mas/pixel$	50 $mas/pixel$	100 $mas/pixel$
J	561 s	276 s	67 s
H	87 s	43 s	11 s
K	26 s	13 s	3 s

Table 3.2: *Integration times per frame for background limited observations*

Filter	J	H	K
Background M [$mag/\square''$]	16.5	14.1	12.4

Table 3.3: *Brightness of the background*

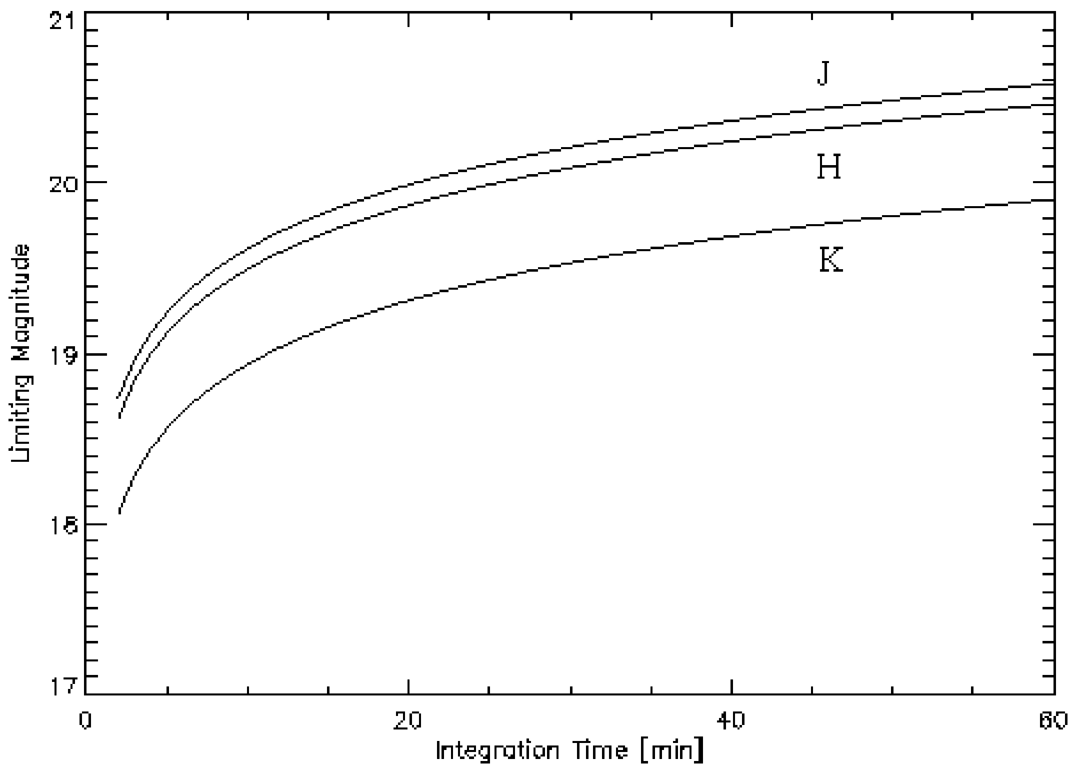

Figure 3.1: *Limiting magnitude for an integration time of one minute per individual frame*

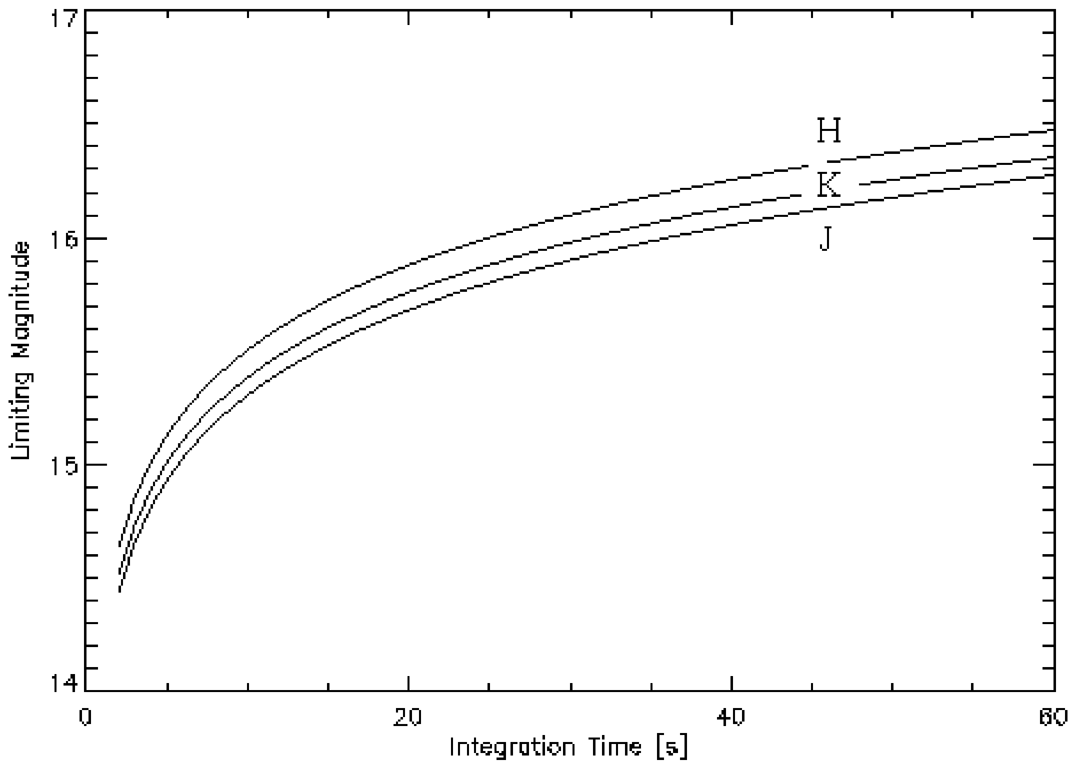

Figure 3.2: *Limiting magnitude for an integration time of one seconds per individual frame*

3.6 Sky subtraction

Because the spatial distribution of the thermal back-round is depending on the position of the adaptive optics ON/OFF mirror, very deep imaging in K-band is limited by residuals ("donuts") from the sky subtraction, when using this ON/OFF mirror for changing from the object to the sky position. To avoid this problem, one should record the sky frames by moving the telescope with the same settings of the ON/OFF mirror.

3.7 Integration time

For standard observations, where the object does not saturate the detector within the shortest integration time of the normal mode (400 ms), this normal mode should be used. For brighter objects, the integrated shutter allows integration times down to 20 ms. Figures 3.3 to 3.5 give a rough estimate of the longest integration time for a point source of given brightness. Because the image correction by the adaptive optics is depending on the seeing conditions, the maximum integration can vary by a factor of about two.

3.8 Spectroscopy

The procedure for spectroscopic observations is similar to that of photometric observations. In both cases one needs to observe object, sky and PSF-reference. Instead of a photometric reference star, now a spectral reference star is necessary. In addition, to determine the line flux, one has to observe the continuum next to the line. Because of the variability of the transmission and emission, best calibration of the data is achieved by frequently observing the reference. Because narrow line observations result in wavelength dependent interference pattern

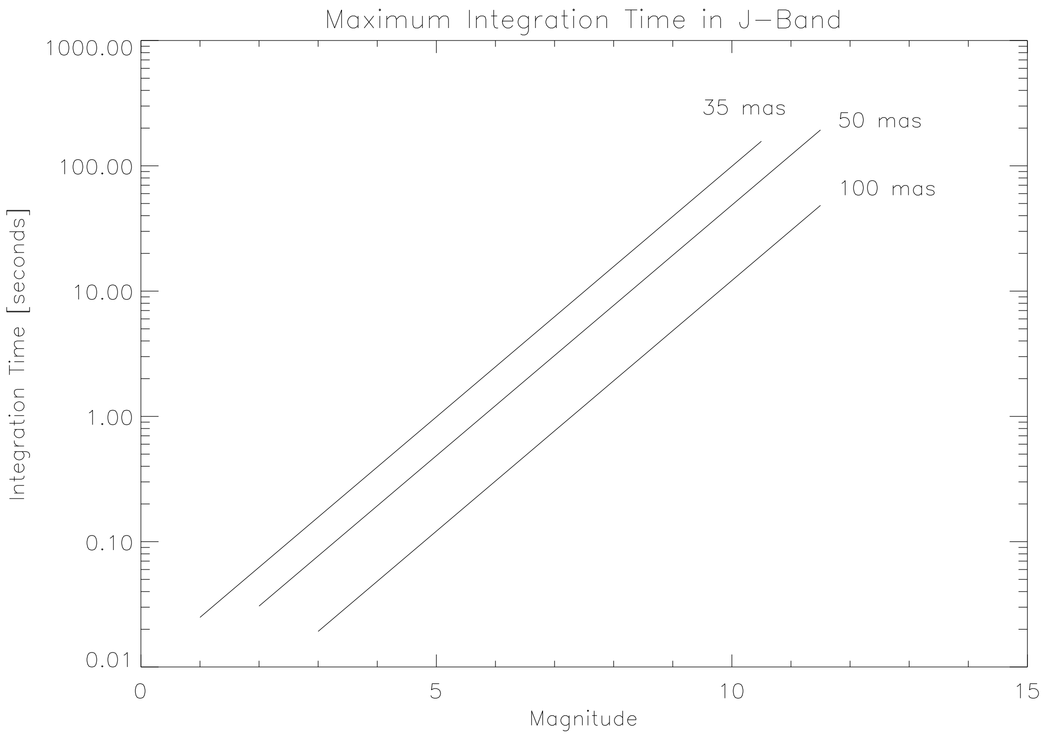

Figure 3.3: *Maximum integration time for given brightness of an object observed in J-band*

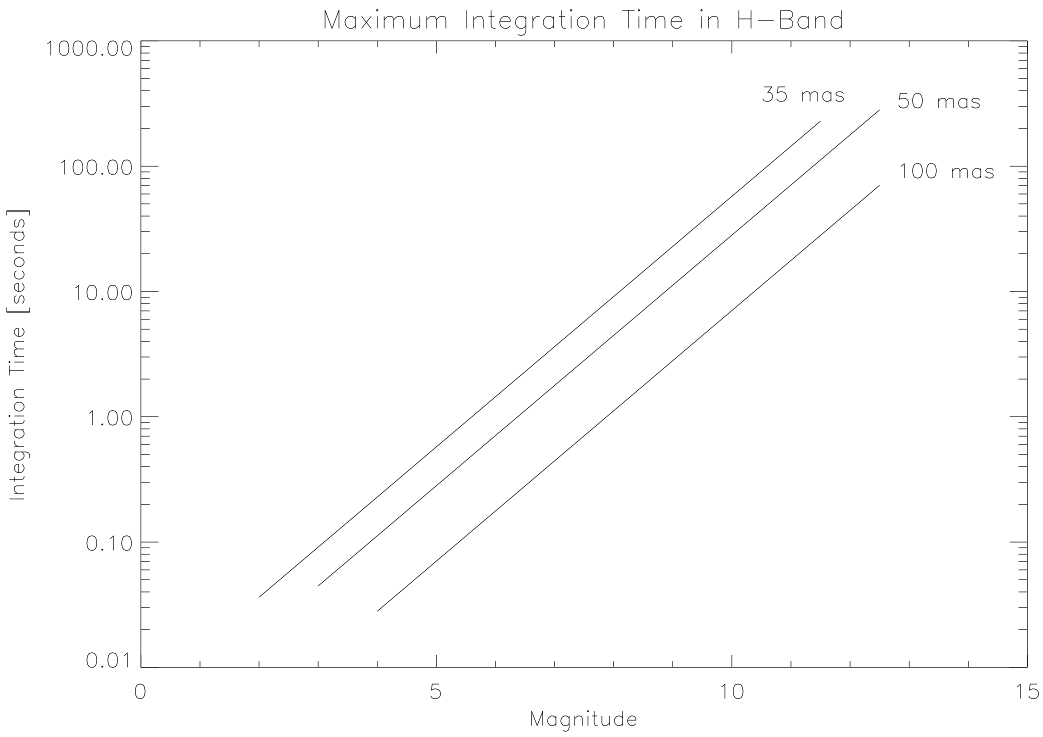

Figure 3.4: *Maximum integration time for given brightness of an object observed in H-band*

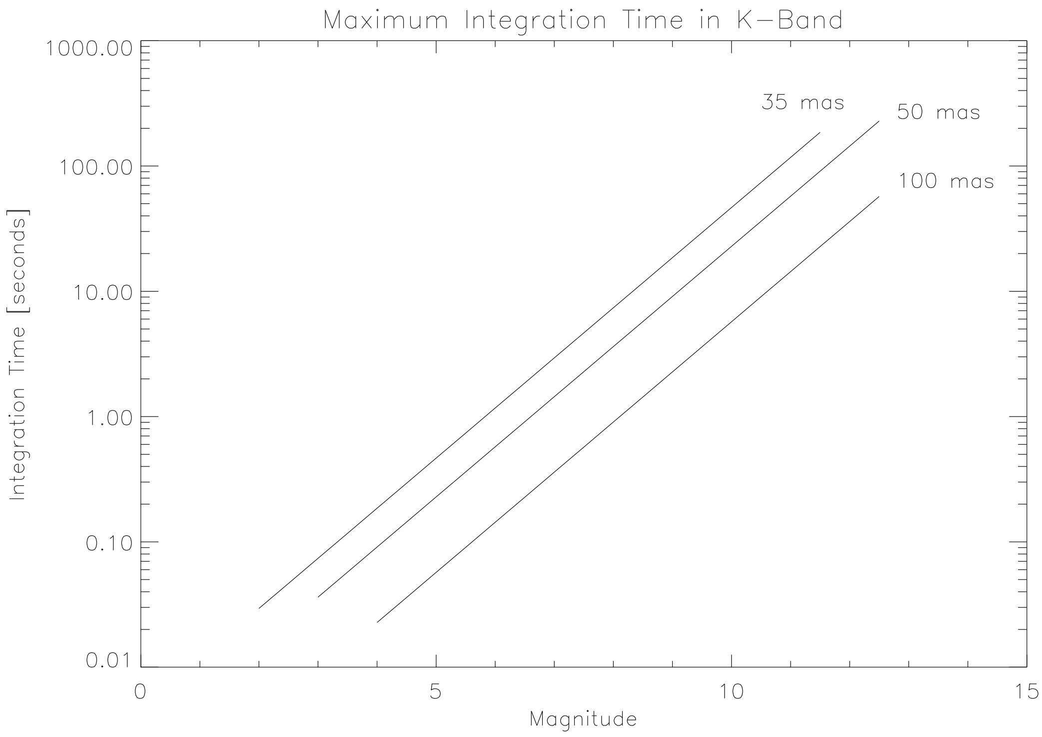

Figure 3.5: *Maximum integration time for given brightness of an object observed in K-band*

(generated by the filter and entrance window of the camera), a separate flat field is necessary for every observed wavelength.

Special remarks on spectroscopy with SHARP II+:

- To minimize lost time between observations of different wavelengths and sky positions, several observing sequences are implemented in the software.
- The 100 *mas/pixel* scale should not be used for spectroscopy. When observing with this pixel scale, there is additional vignetting at the northern edge of the field of view. Also the shift in passband across the filed of view has to be considered, when using the Fabry-Perot etalons.
- Only one of the two Fabry-Perot etalons should be used per night. The procedure for changing the Fabry-Perot etalon requires about half an hour and the support from ESO staff.
- The Fabry-Perot etalons have to be placed manually in the beam.

3.9 Polarimetry

Very similar to spectroscopic observations, where a spectroscopic reference star must be observed along with the object of interest, polarimetry calibrations require observations of an unpolarized reference star. The polarizer has to be placed manually into the beam. Along with the rotation of the polarizer, there is a small shift of the object across the field.

Chapter 4

Examples

4.1 Observations of bright and isolated objects

Nearby guide star

Set the integration per frame to the value showed in the figures 3.3 to 3.5 and check for saturation effects (Linearity range is 21800 ADU). Use the ON/OFF mirror for switching between object, reference star and sky. If the reference star is not within the object frame, record only few frames (about 10) per ON/OFF setting, because the shape of the point spread function can vary rapidly. Remember, that at least one frame is lost when moving the ON/OFF mirror. To avoid memory effects, increase number of wait frames when moving the ON/OFF mirror, or throw away the bad frames afterwards (recommended).

Self-referenced object

The object and its sky is observed as described before, but for deconvolution, a separate star for evaluating the point spread function (PSF) has to be observed. It should be of about the same brightness and color as the object and as close as possible. Because the telescope has to be moved each time when switching from the object to the PSF reference, there will be a big loss in effective integration time (few minutes per telescope movement). But one should not hesitate to spend this time for well calibrated data. The observation of the PSF reference is carried out in the same way as the object.

4.2 Observations of crowded fields

Separate sky observations

Move the telescope to different object free positions in the sky (some arc-minutes from the object). This is somewhat time consuming, but it offers the best sky frames.

Sky subtraction with object frames

If the object field is not extremely covered by sources, one can achieve reasonable sky frames from a mosaic of object frames. Move the ON/OFF mirror in steps of few arc seconds across the region of interest and use the median or minimum (for each individual pixel) as your general sky frame.

4.3 Observations of very faint objects

If you want to detect or image objects at the detection limit of the system (about 19^{th} to 20^{th} Magnitude), accurate sky subtraction is the most important factor. Because of the different thermal background for different ON/OFF mirror position, one necessarily has to observe the sky frame by moving the telescope with non changes in the ON/OFF mirror setting. To avoid large variations in the sky intensity, one should record sky frames at least every few minutes. Because one looses some time when moving the telescope, the effective integration time on the object drops. The best time per object-sky cycle is therefore always a compromise between quality of the sky subtraction and the loss in integration time. The situation is even worse, if separate observations of the PSF reference are necessary, because the shape of the PSF varies faster than the sky emission.

4.4 Recording flat fields

Twilight flat-fields

One way to produce good flat-fields are observations of the sky during twilight (recommended). For each image scale and wavelength used in your observations, record a series of images at a constant integration time, while the brightness of the sky is increasing (dawn) or decreasing (sunset). The root mean square in every pixel will give you its relative efficiency. Normalization of the resulting rms-frame (median or average) will return the flat-field. When recording flat-fields with the Fabry-Perot etalons, it will be necessary to observe the sky about 1 hour before sunset or 1 hour after sunrise. ESO staff will help you to setup a batch file for automatic frame recording.

Dome flat-fields

Very similar to the procedure described before, one can record flat-fields by observing the illuminated dome. Record several frames at the same integration time and with different illumination.

Sky flat-fields

Because in K-band the night sky is bright enough to illuminate the detector sufficient for a high signal to noise flat-field, some instruments can be calibrated by a dark subtracted (filter closed) sky frame. We do not recommend this method for the ADONIS/SHARPII+ system, because of the nonuniform thermal background.

Appendix A

Transmission curves of the filters

Figure A.1: *Transmission-curve of the J-band filter at a temperature of* 77 K

Figure A.2: *Transmission-curve of the H-band filter at a temperature of* 77 *K*

Figure A.3: *Transmission-curve of the K-band filter at a temperature of* 77 *K*

Figure A.4: *Transmission-curve of the K'-band filter at a temperature of* 77 *K*

Figure A.5: *Transmission-curve of the narrow-band filter with a wavelength of* 1068 *nm*

Figure A.6: *Transmission-curve of the HeI narrow-band filter*

Figure A.7: *Transmissioncurve of the $P\gamma$ narrow-band filter*

Figure A.8: *Transmissioncurve of the narrow-band filter with a wavelength of* 1107 *nm*

Figure A.9: *Transmissioncurve of the narrow-band filter with a wavelength of* 1223 *nm*

Figure A.10: *Transmissioncurve of the OII narrow-band filter*

Figure A.11: *Transmissioncurve of the FeII narrow-band filter*

Figure A.12: *Transmissioncurve of the $P\beta$ narrow-band filter*

Figure A.13: *Transmissioncurve of the narrow-band filter with a wavelength of* 1298 *nm*

Figure A.14: *Transmissioncurve of the narrow-band filter with a wavelength of* 2042 *nm*

Figure A.15: *Transmissioncurve of the HeI narrow filter*

Figure A.16: *Transmissioncurve of the narrow-band filter with a wavelength of* 2085 *nm*

Figure A.17: *Transmissioncurve of the narrow-band filter with a wavelength of* 2100 *nm*

Figure A.18: *Transmissioncurve of the* H_2 $\nu : 1 - 0$ *narrow-band filter*

Figure A.19: *Transmissioncurve of the narrow-band filter with a wavelength of* 2144 *nm*